JOURNAL OF ADVANCED TRANSPORTATION
J. Adv. Transp. 2013; **47**:475–482
Published online 30 December 2011 in Wiley Online Library (wileyonlinelibrary.com). DOI: 10.1002/atr.178

An improved car-following model for railway traffic

KePing Li* and ZiYou Gao

State Key Laboratory of Rail Traffic control and safety, Beijing Jiaotong University, Beijing 100044, China

SUMMARY

In this paper, we propose an improved traffic model for simulating train movement in railway traffic. The proposed model is based on optimal velocity car-following model. In order to test the proposed model, we use it to simulate the train movement with fixed-block system. In simulations, we analyze and discuss the space–time diagram of railway traffic flow and the trajectories of train movement. Simulation results demonstrate that the proposed model can be successfully used for simulating the train movement in railway traffic. From the space–time diagram, we find some complex phenomena of train flow, which are observed in real railway traffic, such as train delays. By analyzing the trajectories of train movement, some dynamic characteristics of trains can be reproduced. Copyright © 2011 John Wiley & Sons, Ltd.

KEY WORDS: train movement; car-following model; train control system

1. INTRODUCTION

With computer, communication, and control technologies developing, some new signaling control systems and automatic train protection equipment are applied in modern railway traffic. Meanwhile, new issues and challenges are arising: how to optimize the utilization of existing resources and how to analyze and evaluate the theoretical control algorithm for train movement. In order to help planners to solve these problems, it is necessary to employ computer-based simulation tools [1]. Recently, a number of studies have been done in this field [2–6]. Among these studies, computer-based simulation models can be classified into three types [1,7], that is, the basic model, the time-based model, and the event-based model. The basic model is a reasonable choice when the length of track conductor loop is small. The time-based approach is easy to design and build, but it makes a high computational demand. The event-based model can save computational effort, but it reduces accuracy. To establish a satisfied simulation model that meets practical requirements becomes more and more important for studying railway traffic.

Car-following model is a famous traffic model in studying road traffic flow, which is a good choice for describing the behavior of individual driver. Car-following model has a long history and has been used to study various traffic phenomena observed in real road traffic [8,9]. Many car-following models have been proposed, including the early car-following models [10–12] and some recent improvements [13–16]. One of the advantages of the car-following model is that the analytical structure in the model can be examined. In 1995, Bando *et al.* [13] proposed an important car-following model, called optimal velocity model, which has attracted much attention. Lately, based on such a model, many works have been done, which extended the original optimal velocity model.

Based on the car-following model proposed by Bando *et al.* [13], in this paper, we suggest an improved car-following model, which is suitable for simulating train movement in railway traffic. Here, some realistic driver behaviors and influences of tracked trains are considered. To our knowledge, this work explicitly shows this effect for car-following model for the first time. The paper

*Correspondence to: KePing Li, State Key Laboratory of Rail Traffic Control and Safety, Beijing Jiaotong University, Beijing 100044, China. E-mail: rtkpli@188.com

is organized as follows: in Section 2, we introduce the optimal velocity car-following model. The principle of train control system is introduced in Section 3. In Section 4, we outline the proposed car-following model. The numerical and analytical results are presented in Section 5. Finally, conclusion of this work is presented in Section 6.

2. OPTIMAL VELOCITY MODEL

The car-following model describes the motion of a vehicle following its leader vehicle without making lane change. In the car-following model, a follower tries to maintain a space gap behind its leader. A classical car-following model was proposed by physicist Pipes [10]. In order to account for time lag, Chandler *et al.* [11] suggested an improved car-following model,

$$\ddot{x}_n(t+T) = \lambda[\dot{x}_{n+1}(t) - \dot{x}_n(t)] \tag{1}$$

Here, $x_n(t)$ is the position of vehicle n at time t, T is a response time lag, and λ is the sensitive coefficient. For a more realistic description, Newell [12] presented the optimal velocity car-following model,

$$\dot{x}_n(t+T) = V^{\mathrm{opt}}(\Delta x_n(t)) \tag{2}$$

Where $V^{\mathrm{opt}}(\Delta x_n(t))$ is called optimal velocity function, and $\Delta x_n(t) = x_{n+1}(t) - x_n(t)$ is the headway of vehicle n at time t. More than 30 years later, Bando *et al.* [13] suggested a famous optimal velocity model.

Using the optimal velocity car-following model, the behavior of a driver is captured by a simple differential equation. According to such a differential equation, the acceleration and the deceleration of a vehicle are mainly dependent on the distance between two successive vehicles and the relaxation time τ. Because the optimal velocity car-following model can be derived analytically and because of its simplicity, it has been widely used. However, in realistic traffic, a driver needs to consider more situations around him or her. In order to reproduce traffic as realistically as possible, some complex models are proposed, but they are at the cost of a large number of parameters, or they lose their realistic properties in deterministic limit. So far, a great amount of efforts has been done to improve the optimal velocity car-following model and make it suitable for simulating various realistic traffics. In this paper, our aim is to improve existing car-following model for railway traffic.

3. THE PRINCIPLE OF THE TRAIN CONTROL SYSTEM

Train control system plays a central role in railway traffic. Usually, it is used to decide how a train accelerates/decelerates under the safety restriction and other considered constraints. Fixed-block system (FBS) is an important train control system in railway traffic, which has been widely used on modern railway for more than 1 century. On a fixed-block equipped system, the track is divided into a number of blocks or discrete areas. The length of blocks depends on the maximum velocity, the braking rate, and the number of signaling aspects. In the FBS scheme, the presence of a train within a physical block is usually detected by the operation of electrical "track circuits." Signaling aspects are switched to allow train movements adjacent to or into vacant blocks as circumstance dictates. At any time, one block of track can only be occupied by no more than one train.

With the FBS, train movement is strongly related to the color of the signaling light in front of it: (i) when the color of signaling light in front of one train is red, this train is not allowed to pass through the site where this signaling light is located; (ii) when the color of signaling light in front of one train is green, this train can travel with the maximum velocity; and (iii) when the color of the signaling light in front of one train is other colors, such as the yellow, this train can only be allowed to travel with limited velocity.

DOI: 10.1002/atr

The train movement control system is used to supervise the train movement velocity according to the positions of other trains, the safety protection distance, the station route, and so on. Here, a key step is on how to determine the relationship curve between the train's allowable velocity and distance. According to the relationship curve, based on the position of the current train, the driver/train equipment decides to accelerate/decelerate. In the proposed model, we attempt to use car-following model to determine such a relationship curve.

4. THE PROPOSED MODEL

In Ref. [13], Bando *et al.* proposed a famous optimal velocity car-following model, which is as follows,

$$\ddot{x}_n(t) = \frac{V^{\mathrm{opt}}(\Delta x_n(t)) - \dot{x}_n(t)}{\tau} \tag{3}$$

Where the optimal velocity function V^{opt} is taken as $V^{\mathrm{opt}}(\Delta x_n(t)) = (v_{\max}/2)\{\tanh[\Delta x_n(t) - x_c] + \tanh[x_c]\}$. x_c is called the safety distance, and $v_{\max}$ is the maximum velocity of vehicles. Based on such a car-following model, we propose a new model for simulating train movement in FBS. In the theory of optimal velocity car-following model, the velocity function V^{opt} represents the driver's desired velocity. In the proposed method, V^{opt} is regarded as the driver's desired velocity in the process of train movement. Here, we improve the optimal velocity function V^{opt} and make it suitable for describing the dynamic characters of train.

In formula (3), $1/\tau$ indicates how strongly the driver responds to the information coming from its leader vehicle. In a road traffic system, the driver directly receives the information from its leader car. However, in a railway traffic system, the driver/train equipment receives relevant information from a control center. In general, the control center needs a period to receive information from other trains and then send relevant information to the current train. Therefore, the relaxation time τ in railway traffic systems is larger than that in road traffic systems.

In an FBS, trains traveling on a same track line do not act directly. The interaction between two successive trains is carried out by the signaling lights among them. Theoretically, the distance between two successive trains is at least larger than the length of one block. Sometimes the following train needs to stop in front of the signaling light, and sometimes it is only allowed to run through the signaling light with a limited velocity. According to the principle of FBS, in this paper, we proposed an improved car-following model for simulating train movement. Here, we chose a three-aspect FBS system as our simulation system. Our improvement is focused on the optimal velocity function presented in formula (3). The new optimal velocity function $V^{\mathrm{opt}}(\Delta x_n(t))$ is defined as follows,

Case 1: If the color of the signaling light in front of train n is green, then

$$V^{\mathrm{opt}}(\Delta x_n(t)) = v_{\max} \tag{4}$$

Case 2: If the color of the signaling light in front of the train n is yellow, then

$$V^{\mathrm{opt}}(\Delta x_n(t)) = (v_y - v_r)\{\tanh[\Delta x_n(t)] + v_r\} \tag{5}$$

Case 3: If the color of the signaling light in front of the train n is red, then

$$V^{\mathrm{opt}}(\Delta x_n(t)) = (v_r/2)\{\tanh[\Delta x_n(t) - sm] + \tanh[sm]\} \tag{6}$$

Here, v_y is the limited velocity under the yellow light condition. v_r is the limited velocity under the red light condition. *sm* is called the safety margin distance in train control system. $\Delta x_n(t)$ is the distance from train n to the signaling light in front of it. Equation (4) is used to determine the allowable velocity of the current train when the color of the signaling light in front of the current train is green. In this case, the current train can travel with the maximum velocity $v_{\max}$. Equation (5) is used to determine the allowable velocity of current the train when the color of the signaling light in front of

DOI: 10.1002/atr

the current train is yellow. As $\Delta x(t)$ is larger, the current train can travel with the limited velocity v_y. However, as $\Delta x(t)$ is smaller, the current train must decelerate. If only the current train passes through the position where its leader signaling light locates, it can travel with the limited velocity v_r. In other words, as $\Delta x(t) = 0$, $V^{opt}(\Delta x(t)) = v_r$. Equation (6) is used to determine the allowable velocity of the current train when the color of the signaling light in front of the current train is red. As $\Delta x(t)$ is larger, the current train can travel with the limited velocity v_r. However, as $\Delta x(t)$ is smaller, the current train is not allowed to pass through the position where its leader signaling light locates. Here, we introduce the parameter *sm* so that if $\Delta x_n(t) = 0$, then $V^{opt}(\Delta x(t)) = 0$.

It should be pointed out that Equations (4–6) are all based on the optimal velocity function $V^{opt}(\Delta x(t))$ defined by Bando *et al.* (i.e., Ref. [13]). From the expression of $V^{opt}(\Delta x(t))$ used in Ref. [3], we can give different expression of $V^{opt}(\Delta x(t))$. When the color of the signaling light in front of train *n* is green, train deceleration can be neglected. In this case, $V^{opt}(\Delta x(t)) = v_{max}$, that is, Equation (4). When the color of the signaling light in front of train *n* is yellow, $x_c = 0$. In this case, we give $V^{opt}(\Delta x_n(t)) = (v_y - v_r)\{\tanh[\Delta x_n(t)] + v_r\}$, that is, Equation (5). When the color of the signaling light in front of train *n* is red, replacing x_c by *sm*, we give $V^{opt}(\Delta x(t)) = (v_r/2)\{\tanh[\Delta x_n(t) - sm] + \tanh[sm]\}$, that is Equation (6).

In the three-aspect FBS, after Equation (4) is executed, the next equation to execute is Equation (4) or Equation (5). After Equation (5) is executed, the next executed equation must be Equation (6). There is no correlation between Equation (4) and Equation (5) or Equation (6). However, between Equation (5) and Equation (6), there exists a joint. In Equation (5), as $\Delta x(t) = 0$, $V^{opt}(\Delta x(t)) = v_r$. In Equation (6), as $\Delta x_n(t)$ is larger, $V^{opt}(\Delta x(t))$ is also taken as $V^{opt}(\Delta x(t)) = v_r$.

The dynamic behavior of train movement near a station is complex. When train *n* prepares to travel into a station, if the station in front of train *n* is occupied by another train, then train *n* must keep away from the station. Otherwise, this train can travel into the station directly. In the former case, the distance between train *n* and the station is at least the length of one block. In the latter case, the optimal velocity V^{opt} is taken as

$$V^{opt}(x_s) = v_{max}[\tanh(coe\, x_s)] \tag{7}$$

x_s is the distance between train *n* and the station. *coe* is an adjustable parameter; it is mainly used to control the acceleration and the deceleration of the train. As train *n* arrives at the station, its velocity is set to zero. After the station dwell time T_d, it leaves the station. Boundary condition used in the proposed method is open: (i) when the color of the first signaling light is green, a train with the velocity v_{max} is created at departure station; this train immediately travels according to the proposed equation model; and (ii) at arrival station, train simply moves out of the system.

5. NUMERICAL SIMULATIONS

We use the proposed equation model to simulate the train movement in FBS. However, formula (3) must be rewritten. At first, by changing the time derivative, the proposed equation is simplified to a discrete formula. Then, we iterate the discrete equation. Basic step is that at each time, for all trains, we use the current velocities and positions of trains to calculate the velocities and sites of these trains at the next time step. The following traffic situations are dealt with the following: (i) rail line has the single-track sections; and (ii) one station is designed at the middle of the system.

The different expressions of optimal velocity functions may lead to the acceleration/deceleration discontinuity, especially the acceleration/deceleration change from Case 1 to Case 2. In order to avoid unrealistic change of train acceleration/deceleration, we need choose a suitable value for the relaxation time τ. For example, when the difference between the chosen values of the parameters in Case 1 and Case 2 is larger, τ should take a larger value. In this case, from formula (3), we can infer that the change of train acceleration/deceleration is small. This ensures that the train velocity changes smoothly. A system of $L = 1000$ is considered, which is divided into 10 blocks. The iteration time step is $T_s = 1000$. The velocities v_{max}, v_y, and v_r are respectively taken as $v_{max} = 10$, $v_y = 6$, and $v_r = 2$. The value of *sm* is set to be $sm = 10$.

In order to investigate some complex phenomena of train flow, we study the space–time diagram of the railway traffic flow. Simulation results indicate that when the station dwell time T_d is large, train

DOI: 10.1002/atr

delays begin to emerge. Figure 1 shows the space–time diagram of a railway traffic flow for $coe = 0.01$. Here, we plot 1000 sites in 500 consecutive time steps. The horizontal direction indicates the direction in which trains move ahead. The vertical direction indicates time. In Figure 1, the positions of trains are indicated by dots. From Figure 1, we can clearly observe the processes of train movements. All trains start from the departure site, that is, the site $l = 1$, and then arrive at the station, that is, the middle site $l = 500$. After the station dwell time T_d, they leave the station. When they arrive at the arrival site, that is, the site $l = 1000$, they leave the system. Before the station, the train delays form and propagate backward. In Figure 1(a), as the simulation evolution proceeds, the train delays disappear, but in Figure 1(b), as the simulation evolution proceeds, the lengths of the delay times increase. The reason is that when τ is small, the accelerations and decelerations of trains are large. In this case, the train delays can quickly propagate backward so that the train delays can be easily reduced.

When a train passes through a station, its dynamic behavior is complex. In this case, it needs to stop to enable passengers to board and alight. Figure 2 shows the local space–time diagram, which displays the positions and velocities of the trains near the station. Here, numbers represent the velocities of trains. The parameters used in the equation model are same as that used in Figure 1(a). From Figure 2, we can clearly see how trains change their velocities and maintain the safety stopping distance among them. In Figure 2, as station P is occupied by train A, train B is not allowed to travel into the first block in front of station P. When train B arrives at the block boundary (i.e., the site $l = 400$), it needs to stop at this boundary. Similarly, train C also stops at the block boundary (i.e., the site $l = 300$). These are the characteristic behaviors of train movements under the FBS condition. In this paper, we focus on the case where the station dwell time is large. Under such a condition, we can observe the complex behavior of train movement.

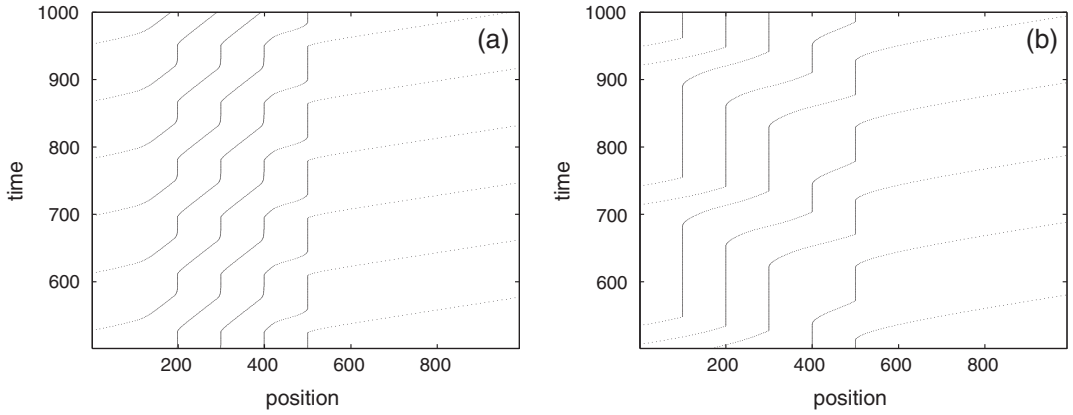

Figure 1. Local space–time diagram of railway traffic flow for $T_d = 50$. (a) $\tau = 5$, (b) $\tau = 10$.

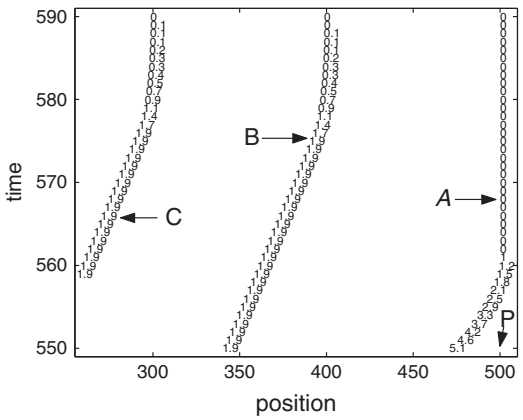

Figure 2. A diagram displaying the positions and velocities of trains.

DOI: 10.1002/atr

Among all the constraints of train movement, safety distance is the most important factor. When the color of the signaling light in front of one train is red, it is not allowed to travel toward the physical block in front of it. One physical block is only occupied by one train. In order to make the train travel smoothly, the distance between two successive trains is at least larger than the length of the physical block. Using the proposed model, we measure the distribution of the distance headway Δs_n. Here, Δs_n is defined as the distance from the current train n to its leader train $n+1$. Figure 3 shows the distribution of the distance headway at the time $t=1000$. Here, the solid line denotes the measurement results, and the dotted line denotes the length of one physical block. At the time $t=1000$, there are four trains traveling on the single line. From Figure 3, it is obvious that the measurement results are all larger than the length of one physical block. In other words, these trains can travel safely.

When a train travels from a departure station to its arrival station, it needs to change its velocity continuously. Sometimes it accelerates or decelerates, and sometimes it travels at the inertia motion. Figure 4 shows how the velocity varies with the simulation time t. Here, this tracked train departs from the site $i=1$ at the time $t=500$. In Figure 4, when the tracked train travels toward the station, sometimes it travels with the limited velocity v_r, and sometimes it stops at a site in front of the station. When the tracked train arrives at the station, its velocity is zero; that is, it stops at the station. After the station dwell time T_d, it accelerates continuously until it has a maximum velocity v_{max}. The simulation results indicate that the proposed model is an effective tool for simulating train movement under the FBS condition.

In railway traffic, train can only decrease (or accelerate) step by step. The deceleration and the acceleration of a train are limited between the region $[-1.5\,\mathrm{m/s^2},\ 2\,\mathrm{m/s^2}]$. Figure 5 presents the accelerations and decelerations of all trains in simulations. From Figure 5, we can see that the

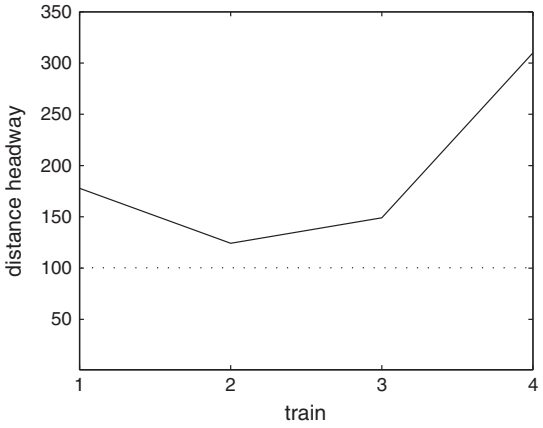

Figure 3. Distribution of the distance headway for $T_d=10$ and $\tau=5$.

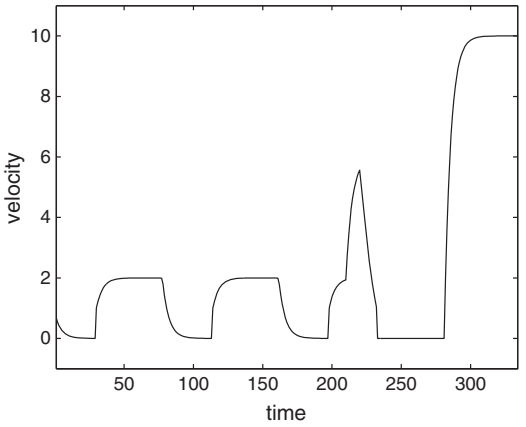

Figure 4. How the velocity of one tracked train varies with the evolution time for $T_d=50$, $\tau=5$, and $coe=0.01$.

DOI: 10.1002/atr

accelerations of all trains are between the region [0 m/s^2, 2 m/s^2], and the decelerations of all trains are between the region [−1.5 m/s^2, 0 m/s^2]. In the proposed equation model, the relaxation time τ can be used to control the region of the acceleration and deceleration. When the parameter τ is small, the region of the acceleration and deceleration is larger. On the contrary, when the parameter τ is large, the region of the acceleration and deceleration is small.

When trains travel toward station, the parameter *coe* expressed in formula (7) is used to change the acceleration/deceleration rate. Figure 6 places how the velocity varies with the simulation time near

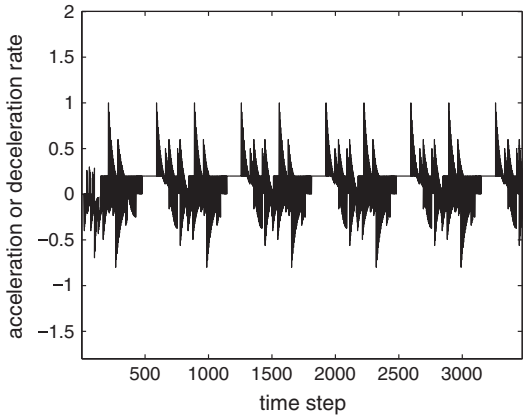

Figure 5. Accelerations and decelerations of all trains for $T_d = 50$, $\tau = 5$, and $coe = 0.01$.

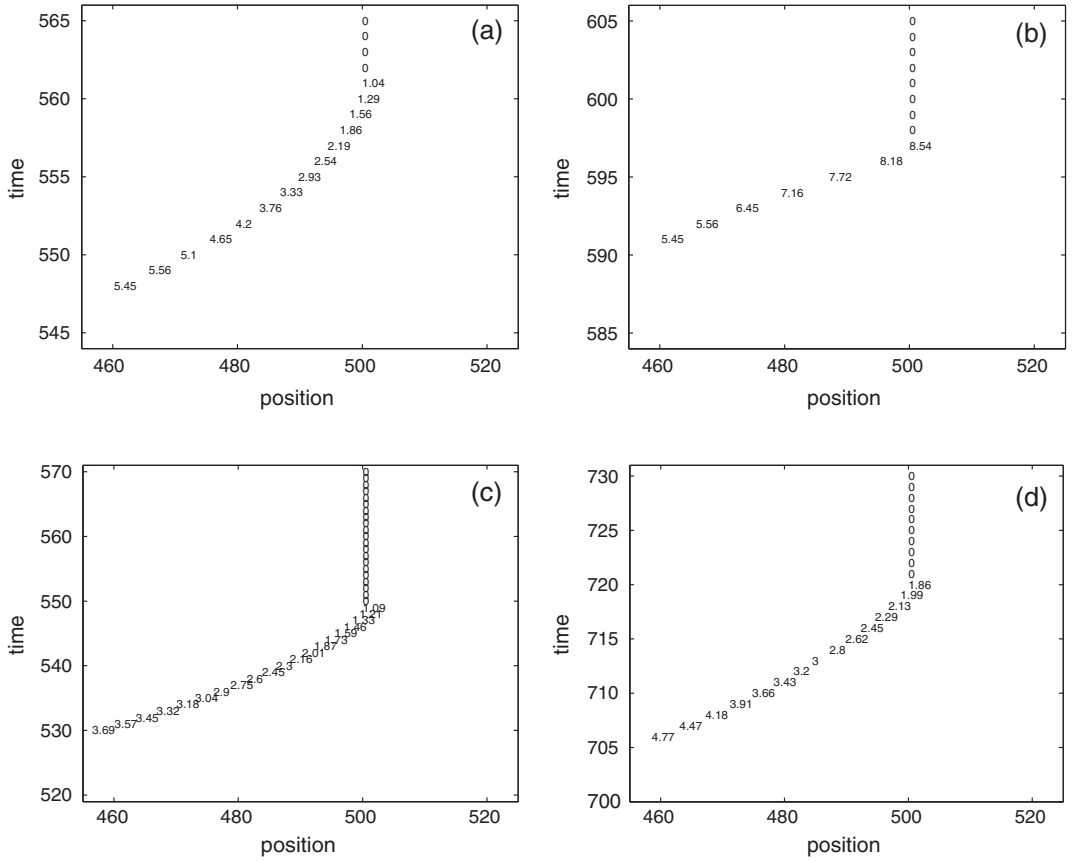

Figure 6. A diagram displaying the positions and velocities for $T_d = 50$. (a) $\tau = 5$ and $coe = 0.01$, (b) $\tau = 5$ and $coe = 1$, (c) $\tau = 10$ and $coe = 0.006$, (d) $\tau = 15$ and $coe = 0.0005$.

DOI: 10.1002/atr

the station. The numerical simulation result shown in Figure 6(a) is obtained for $coe = 0.01$, and the result shown in Figure 6(b) is obtained for $coe = 1$. Comparing Figure 6(a) with Figure 6(b), we can obviously see that the train decreases gradually in Figure 6(a), but it decreases abruptly in Figure 6(b). For different values of parameter τ, we need to select a reasonable value of *coe*. When τ is larger, *coe* should take a smaller value. On the contrary, when $v_{\max}$ is smaller, *coe* can take a larger value. Figure 6(c) and Figure 6(d) show the results for various τ and *coe*.

6. CONCLUSIONS

In conclusion, an improved optimal velocity car-following model is used for simulating train movement in FBS. After such an improved model is discretized, we iterated it to simulate the train movement under open boundary condition. The numerical simulation results indicate that the proposed model can well describe the train movement in FBS. The proposed equation model provides a new approach to further analyze and evaluate the theoretical control algorithm of train control systems.

However, the traffic situations considered in this paper are simplified. In real railway traffic, rail lines have double-track sections, stations have several platforms, and there are at least two types of trains traveling on the same rail line. In addition, train movement is affected by other trains, which come from other track sections. In fact, these problems can be solved by modifying the basic traffic situation. We think that the proposed equation model is worthy of further study.

ACKNOWLEDGEMENTS

The project is supported by the National Natural Science Foundation of China under Grant Nos 60634010 and 60776829 and the State Key Laboratory of Rail Traffic Control and Safety (Contract Nos. RCS2008ZZ001 and RCS2010ZZ001), Beijing Jiaotong University.

REFERENCES

1. Goodman CJ, Siu LK, Ho TK. A review of simulation models for railway system. In *International Conference on Developments in Mass Transit Systems*. IEEE Computer Society: Washington, DC, 1998; 80–85.
2. Petar K, Guedial S. Minimum-energy control of a traction motor. *IEEE Transactions on Automatic Control* 1972; **17**:92–95.
3. Howlett PG, Cheng J. Optimal driving strategies for a train on a track with continuously varying gradient. *Journal of the Australian Mathematical Society, Series B* 1997; **38**:388–411.
4. Cheng J, Davydova Y, Howlett P, Pudney P. Optimal driving strategies for a train journey with non-zero track gradient and speed limits. *IMA Journal of Mathematics Applied in Business and Industry* 1999; **10**:89–115.
5. Liu R, Golovitcher IM. Energy-efficient operation of rail vehicles. *Transportation Research. Part A* 2003; **37**:917–932.
6. Howlett P. The optimal control of a train. *Annals of Operations Research* 2000; **98**:65–87.
7. Ho TK, Mao BH, Yang ZX. A muti-train movement simulator with moving block system. In *Computers in Railways VI*. WIT Press: Lisbon, 1998; 782.
8. Komatasu T, Sasa S. Kink soliton characterizing traffic congestion. *Physical Review. E* 1995; **52**:5574–5582.
9. Nagatani T. Stabilization and enhancement of traffic flow by the next-nearest-neighbor interaction. *Physical Review. E* 1999; **60**:6395–6410.
10. Pipes LA. An operational analysis of traffic dynamics. *Journal of Applied Physics* 1953; **24**:274–287.
11. Chandler RE, Herman R, Montroll EW. Traffic dynamics: studies in car following. *Operational Research* 1958; **6**:165–184.
12. Newell GF. Nonlinear effects in the dynamics of car following. *Operational Research* 1961; **9**:209–229.
13. Bando M, Hasebe K, Nakayama A. Dynamical model of traffic congestion and numerical simulation. *Physical Review. E* 1995; **51**:1035–1042.
14. Helbing D, Tilch B. Generalized force model of traffic dynamics. *Physical Review. E* 1998; **58**:133–138.
15. Treiber M, Hennecke A, Helbing D. Congested traffic states in empirical observations and microscopic simulations. *Physical Review. E* 2000; **62**:1805–1824.
16. Tomer E, Safonov L, Havlin S. Presence of many stable nonhomogeneous states in an inertial car-following model. *Physical Review Letters* 2000; **84**:382–385.

DOI: 10.1002/atr